

Development of a Fluoride-Selective Electrode based on Scandium(III) Octaethylporphyrin in a Plasticized Polymeric Membrane

Youngjea Kang, Christopher Lutz,[†] Sung A Hong, Dayeon Sung, Jae Seon Lee, Jae Ho Shin, Hakhyun Nam, Geun Sig Cha,^{*} and Mark E. Meyerhoff^{‡*}

Department of Chemistry, Kwangwoon University, Seoul 139-701, Korea. *E-mail: gscha@kw.ac.kr

[†]Department of Chemistry, University of Wisconsin-Stout, Menomonie, WI 54751, U.S.A.

[‡]Department of Chemistry, University of Michigan, Ann Arbor, MI 48109, U.S.A. *E-mail: mmeyerho@umich.edu

Received April 3, 2010, Accepted April 20, 2010

A scandium(III) porphyrin-based fluoride-selective potentiometric sensor and its application in the analysis of hydrofluoric acid is described. Scandium(III) octaethylporphyrin, an ionophore recently developed for the optical fluoride sensor, was employed as a host molecule for the selective binding with fluoride in the plasticized PVC membrane. Nernstian response for F⁻ between 10^{-4.6} to 10⁻¹ M was observed at a glycine-phosphate buffer (pH 3.0). The selectivity pattern was observed as F⁻, salicylate >> SCN⁻ > Cl⁻, Br⁻, NO₃⁻, ClO₄⁻, which is consistent with the binding constant data measured in the plasticized PVC membrane based on a sandwich membrane method. This highly selective and reversible fluoride-sensitive electrode was employed for the analysis of hydrofluoric acid (HF). A disposable differential-type HF sensor was fabricated on the screen-printed electrode and demonstrated its ability to detect the neutral HF in the acidic solution.

Key Words: Fluoride sensor, Hydrofluoric acid gas sensor, Ion-selective electrode, Scandium porphyrin

Introduction

Fluoride is one of the most important ionic species in drinking water.^{1,2} It is also product of enzymatic reactions of nerve gases such as soman and sarin and the measurement of fluoride from such reactions can be used for the detection of toxic organic fluorophosphates.^{3,4} While the solid state electrode based on the LaF₃ crystal is widely employed for many field applications, the development of an inexpensive fluoride sensing device has gained considerable interest among sensor scientists and, as a result, highly selective ionophores for fluoride have been recently developed for electrochemical and optical sensors based on plasticized polymeric matrices.

Fluoride had been one of the most difficult anions detected by sensors made of the organic polymeric matrices due to its highly negative Gibbs free energy of hydration (-104 kcal/mol).⁵ Beginning from gallium(III) porphyrins,⁶ many organometallic species have been found to bind strongly yet reversibly with fluoride; Zr(IV) porphyrins,^{7,8} schiff-base complexes of Ga(III)⁹ or Zr(IV),¹⁰ and Al(III) porphyrins¹¹⁻¹⁵ have all been studied to create new fluoride sensors. Among them, Al(III) complexes provide best selectivity for fluoride. Meanwhile, Sc(III)OEP has recently been reported for an optical sensor with an excellent selectivity for fluoride that is comparable to the Al(III)-based ionophores.¹⁶ In addition, unlike Al(III) porphyrins, the observation of a novel fluoro-bridged dimer led to a better understanding on its response mechanism. The promising result with the optical sensor based on Sc(III)OEP strongly suggests that an ion-selective electrode prepared with this ionophore should provide the similar selective response pattern for fluoride.

In this work, a fluoride-selective electrode based on Sc(III)-OEP in a plasticized PVC film is characterized in terms of selectivity, reversibility, lifetime, and response mechanism. Binding

constants of Sc(III)OEP with various anions in the plasticized film are also determined. The detection of gaseous hydrofluoric acid (HF) is further demonstrated with the Sc(III)OEP-based ion-selective electrode using a novel differential measurement configuration.

Experimental

Reagents. Hydroxo(2,3,7,8,12,13,17,18-octaethylporphyrinato) scandium(III) (Sc(III)OEP-OH) was prepared according to previous literature reports.^{17,18} Tridodecylmethylammonium chloride (TDMACl), potassium tetrakis(*p*-chlorophenyl) borate (KTpCIPB), potassium tetrakis(3,5-trifluoromethyl-phenyl) borate (KTFPB), high molecular weight poly(vinyl chloride) (PVC), di(tridecyl) adipate (DTDA), *o*-nitrophenyl octyl ether (*o*-NPOE), and bis(2-ethylhexyl) sebacate (DOS) were used as received from Fluka (Ronkonkoma, NY). Tetrahydrofuran (THF) was from Sigma-Aldrich (St. Louis, MO) and distilled before use. Glycine and citric acid were obtained from Fisher Scientific (Cincinnati, OH). Sodium salts of anions (bromide, chloride, nitrate, perchlorate, phosphate monobasic, salicylate, and thiocyanate) were obtained from Sigma-Aldrich.

Membrane preparation. Membrane cocktails were prepared by dissolving Sc(III)OEP-OH (1.0 mg), lipophilic ionic sites (i.e., KTpCIPB, KTFPB, or TMDACl) (0 ~ 60 mol % relative to Sc(III)OEP-OH), a plasticizer (66 mg), and PVC (33 mg) in 5 mL THF. Membranes were prepared by casting the membrane cocktail in a glass o-ring (i.d. = 22 mm) affixed on the glass slides (75 mm × 50 mm × 1 mm). The membrane was dried overnight in the dark, and 8 mm-diameter disks were cut to prepare the membrane electrodes. The electrodes were conditioned in the buffer (0.05 M glycine-phosphate, pH 3.0) for 8 h before use. The membranes should be kept in the dark to minimize any loss

via photo-decomposition.

Electrochemical studies. Ion-selective electrodes based on Sc(III)OEP-doped plasticized membranes were prepared using electrode bodies (Oesch Sensor Technology, Sargans, Switzerland). The galvanic cell employed in this work consisted of: Ag/AgCl(s), KCl (4 M)(aq)/LOAc (1 M)(aq)/sample solution/membrane/internal solution, AgCl(s)/Ag. Potential responses of the sensors were measured by a high impedance voltmeter (VF-4, World Precision Instruments) connected to a personal computer running Labview software (version 7.0, National Instruments). The internal solution was prepared by dissolving NaCl (10 mM) and NaF (10 mM) in the glycine-phosphate buffer (0.05 M, pH 3.0). All the EMF responses were correlated to anion activities that were calculated based on the two-parameter Debye-Hückel method.¹⁹ For most experiments, a 0.05 M glycine-phosphate buffer (pH 3.0) was used as the background electrolyte. Anion solutions were prepared by dissolving corresponding sodium salts in the same buffer. A stock fluoride solution (1 M) was prepared by dilution of hydrofluoric acid solution with the buffer and the pH was adjusted to *ca.* pH 3.0 by addition of sodium hydroxide.

Optical studies. Spectra of Sc(III)OEP in the plasticized film were monitored with a UV-vis spectrophotometer (model Lambda 35; Perkin-Elmer, Boston, MA). A thin film (*ca.* 1 μm thickness) was prepared on a glass slide and this glass slide was bathed within the buffer solution in the quartz cuvette during the measurement.

Analysis of HF. The screen-printed electrodes were made of insulating layers and a silver layer on PET substrates (polyethylene terephthalate, acryl coated, 250 μm thick), which were fabricated using a LS-150 semi-automatic screen-printer (Tokyo, Japan). The silver electrode was oxidized by a FeCl₃ solution (0.3 M). A cocktail solution of hydrogel consisted of citric acid (0.1 M), NaCl (1.0 M), and PVP90K (0.1 wt %). The pH of this solution was adjusted by addition of appropriate amount of the NaOH solution. The hydrogel layer was formed on the Ag/AgCl electrode on the PET substrate by dispensing the cocktail solu-

tion with a pneumatic dispensing instrument (EFD model 1000 XL; Providence, RI, USA). The sensor membrane was dispensed on the dried hydrogel layer and kept in the dark place for a day before use. The differential sensor consists of a working electrode whose PVC : *o*-NPOE ratio was 1:2 and a reference electrode whose PVC : *o*-NPOE ratio is 2:1. The membrane was conditioned in the NaCl solution (1 M in deionized water) for 10 min and then dipped into the HF solution. The signal was obtained at 180 s after dipping. The potential of each working and reference electrode was measured separately and then the difference was calculated.

Results and Discussion

Selectivity and response mechanism. In general, the boundary potential developed at the interface across the aqueous phase and membrane phase is described by:

$$E_{\text{mem}} = E_{\text{const}} - S \cdot \log \left(\frac{a_{X^-}}{[X^-]_{\text{mem}}} \right) \quad (1)$$

where E_{mem} , E_{const} , and S are the overall membrane potential, the potential term independent on activities of analytes in the sample phase, and the response slope, respectively. The activity of analyte anion (X^-) in the sample phase is denoted by a_{X^-} and the concentration of the analyte anion in the membrane phase is expressed in $[X^-]_{\text{mem}}$. In order for the signal to be dependant only on the activity of anion in the sample phase, $[X^-]_{\text{mem}}$ should remain constant during activity changes of X^- in the sample phase. For example, a certain amount of the lipophilic anion exchanger (or cationic additives) such as tridodecylmethylammonium (i.e., TDMA⁺) can be incorporated in the membrane so that the concentration of anion in the membrane should be equal to the concentration of TDMA⁺ due to the neutrality condition. In the case of ionophore-based anion-selective electrodes, the complexation reaction between an ionophore (L) and the analyte anion

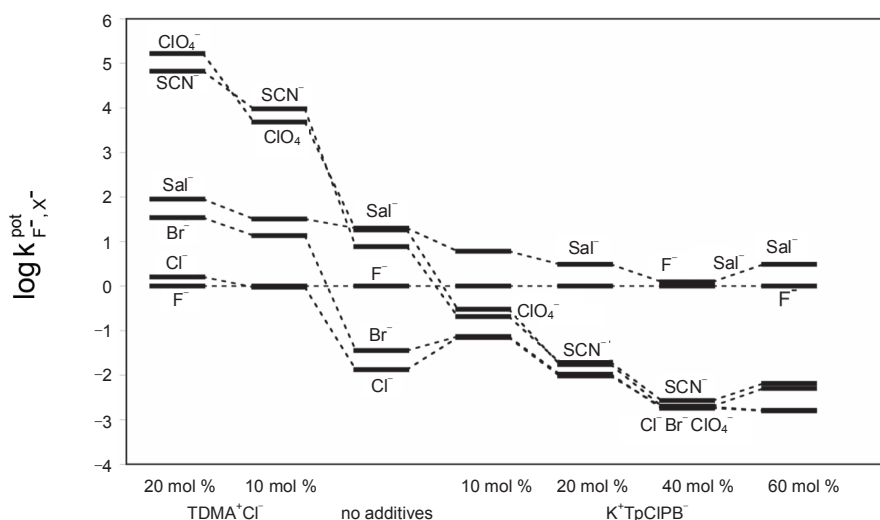


Figure 1. Potentiometric selectivity coefficients for various anions (relative to fluoride) with varying amount of ionic additives in the polymer membrane (Sc(III)OEP-OH (1 mg)/ TDMACl or KTpCIPB/*o*-NPOE (66 mg)/PVC (33 mg)).

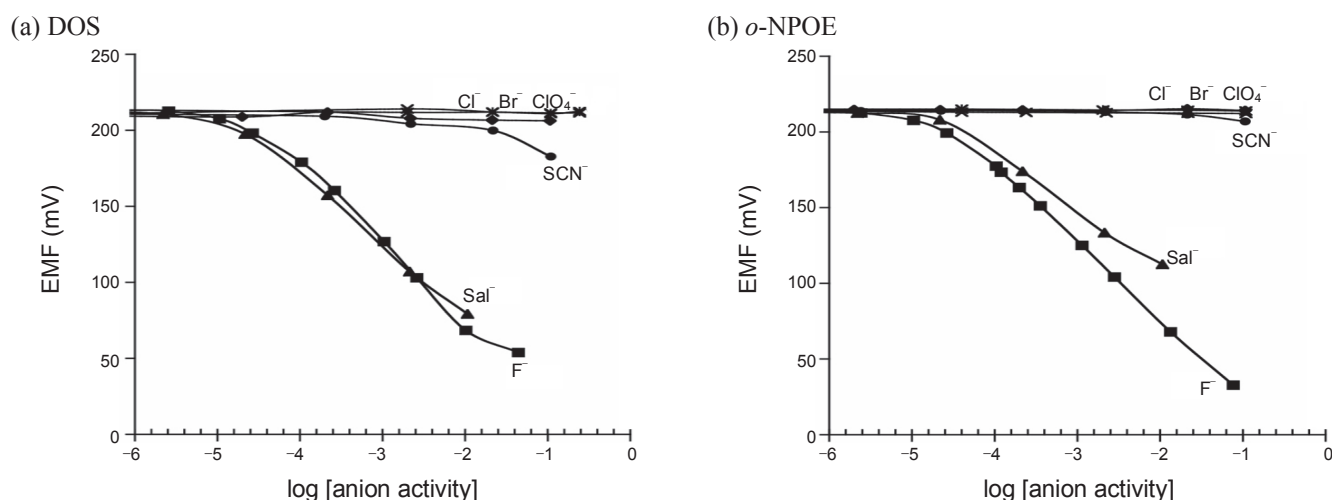


Figure 2. Response curves of fluoride-selective electrodes based on Sc(III)OEP containing 40 mol % KTFPB in plasticized (a) DOS and (b) *o*-NPOE PVC membranes.

(X) minimizes the change of $[X^-]_{\text{mem}}$. Two distinctive mechanisms are known in such ionophore-based sensors: the neutral carrier mechanism and the charged-carrier mechanism. In the neutral carrier mechanism, the unligated ionophore is a neutral species that requires lipophilic cationic sites (e.g., TDMA⁺) to stabilize the anion-ionophore complex. On the other hand, in the charged carrier mechanism, the complex of anion and ionophore is neutral and the unligated ionophore is cationic. Therefore, lipophilic anionic additives such as lipophilic tetraphenylborate derivatives are required to exhibit an optimal anionic response.²⁰

Figure 1 illustrates the potentiometric selectivity change as the amount of ionic sites are varied in the plasticized film doped with Sc(III)OEP. Increasing anionic sites up to 40 mol % improves the potentiometric selectivity coefficient for fluoride over other anions. With the cationic additive or TDMA⁺, the effect of ionophore is minimal and the selectivity pattern follows the classical Hofmeister selectivity series. As the TDMA⁺ is removed and the anionic additive or TpCIPB⁻ is incorporated, responses for lipophilic anions (i.e., ClO₄⁻, SCN⁻) are dramatically reduced compared to that of fluoride. Responses for chloride and bromide are slightly improved at 10 mol % TpCIPB⁻, but reduced after 20 mol % TpCIPB⁻. The selectivity for fluoride is optimal at 40 mol % TpCIPB⁻ in the membrane phase. Therefore, these results are consistent with a charged carrier mechanism, where the lipophilic anionic additive is required for the optimal performance. The following equilibrium determines the free ion concentration of F⁻ in the membrane:



where L⁺ and LF indicate the unligated ionophore (i.e., Sc(III)OEP⁺) and fluoro-complex (i.e., Sc(III)OEP-F) in the membrane phase. The free ionic concentration of fluoride in the membrane is determined by the equation:

$$\beta = \frac{[LF]_{\text{mem}}}{[L^+]_{\text{mem}}[F^-]_{\text{mem}}} \quad (3)$$

where β is the equilibrium constant of reaction (2) or the anion binding constant. When the membrane potential (E_{mem}) in Eq. (1) is dependent on the a_{F^-} , $[F^-]_{\text{mem}}$ should be constant in both Eq. (1) and (3) as activity of fluoride in the sample changes. If the binding constant (β) is high enough, the concentration of free fluoride in the membrane is usually much less than that of lipophilic anionic sites, and thus the concentration of L⁺ is approximately equal to that of anionic sites (i.e., TFPB⁻ or TpCIPB⁻). Because the total concentration of ionophore ($[L^+] + [LF]$) and the concentration of the cationic form ($[L^+]$) are constant, the concentration of the ligated form (LF) should be also constant. Therefore, every term in the Eq. (3) is constant including $[F^-]_{\text{mem}}$. In this way, the charged carrier mechanism ensures that the change of membrane potential, E_{mem} , should be dependant only on the activity of fluoride in the sample phase in Eq. (1).

At the optimized condition (i.e., 40 mol % of KTFPB), the calibration curves for the anions tested are shown in Fig. 2. The selectivity sequence of the Sc(III)OEP based membrane is $F^- \sim \text{Sal}^- \gg \text{SCN}^- > \text{Cl}^-, \text{Br}^-, \text{NO}_3^-, \text{ClO}_4^-$. This pattern is clearly the same as the selectivity pattern observed in the optical sensors based on Sc(III)OEP along with ETH 7075.¹⁶ The response slope is slightly sub-Nernstian (51.9 mV/decade (*o*-NPOE) and 56.5 mV/decade (DOS)) in the linear response range ($10^{-4} \sim 10^{-2}$ M). In general, since metalloporphyrin-based anion sensors are experiencing hydroxide interference, the pH of the sample solution should be lowered to minimize the OH⁻ interference and to lower the detection limit.^{6,7,21} For the fluoride sensor, pH 3.0 is chosen as the preferred pH for the fluoride measurement since a pH lower than 3.0 turns fluoride nearly completely to the neutral HF (pK_a 3.17). The detection limit for fluoride at pH 3.0 is about 1.9×10^{-5} M (using *o*-NPOE as plasticizer) and 2.6×10^{-5} M (DOS).

Reversibility and lifetime. In Figure 3, reversibility tests with membranes of Sc(III)OEP/KTFPB (40 mol %)/plasticizer (either *o*-NPOE or DOS)/PVC clearly indicates fast and reproducible EMF responses toward fluoride. The potentiometric response to either higher fluoride concentrations (10^{-2} M) or lower

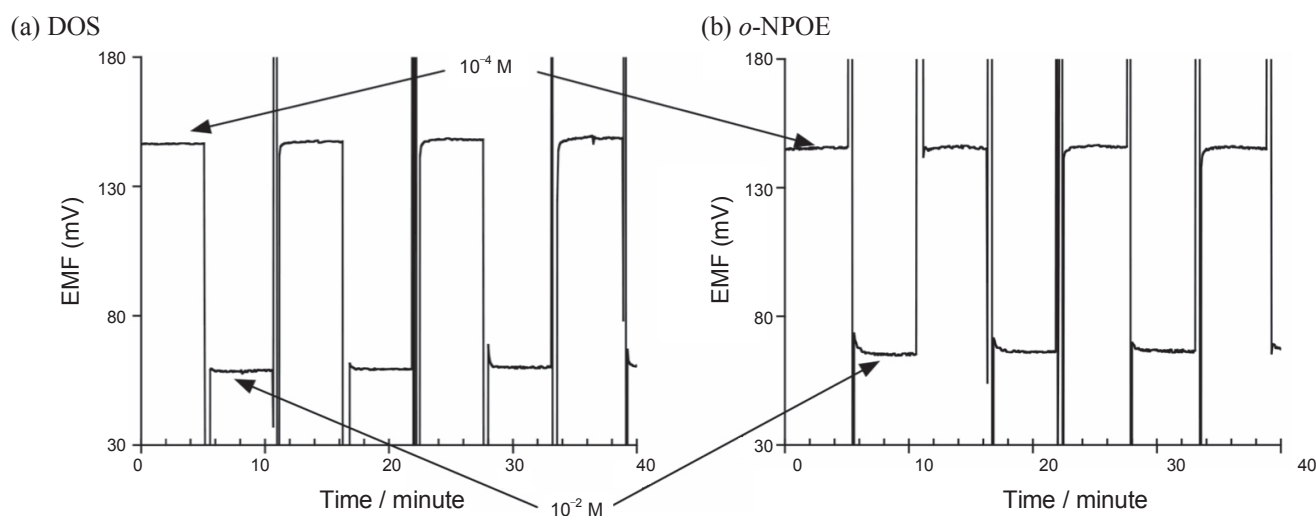


Figure 3. EMF responses of fluoride-selective electrodes using a film composed of Sc(III)OEP/KTpCIPB (40 mol%)/DOS (a) or *o*-NPOE (b)/PVC between 0.01 M and 0.0001 M fluoride solutions.

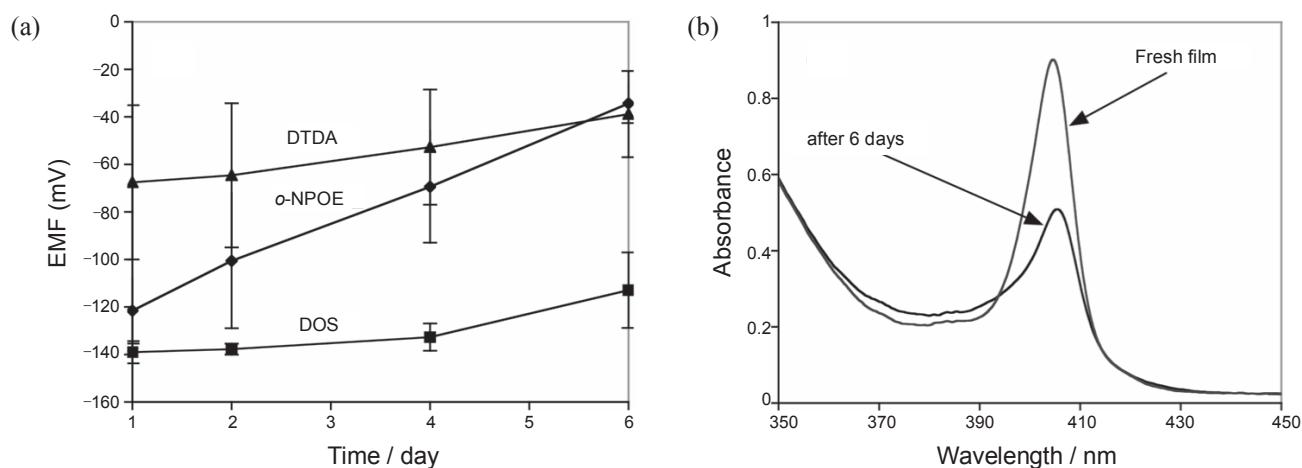


Figure 4. (a) Change in EMF response to 0.01 M fluoride over time with films (Sc(III)OEP/KTFPB (40 mol%)/plasticizer (DTDA or *o*-NPOE or DOS)/PVC). (b) UV-vis spectra of the PVC film plasticized with *o*-NPOE before and after lifetime experiment.

concentrations (10^{-4} M) requires about 10 sec to stabilize. As can be seen in Fig. 4(a), an experiment aimed at assessing the lifetime of the film (Sc(III)OEP-OH/KTFPB (40 mol %)/*o*-NPOE/PVC) showed a significant potential drift. The decrease of the Soret band in Fig. 4(b) suggests a loss of Sc(III)OEP is likely the main cause of the deterioration of EMF response when the film is stored in 0.05 M glycine-phosphate buffer (pH 3.0) for six days. Employing plasticizers with low dielectric constant such as DOS ($\epsilon = 3.9$)²² and DTDA ($\epsilon = 2.5 \sim 2.6$)^{23,24} rather than with *o*-NPOE ($\epsilon = 23.9$)²² has minimized the deterioration of responses over time.

Binding constants. The sandwich membrane method^{25,26} was employed to determine the binding constants of the anions with Sc(III)OEP in the plasticized PVC film contacting the aqueous phase and the results of these experiments are summarized in Table 1. As expected from the observed potentiometric selectivi-

Table 1. Binding constants (β) of Sc(III)OEP with various anions as determined by measuring voltages across sandwich of membranes (Sc(III)OEP-OH (1.0 mg)/KTpCIPB (40 mol %)/*o*-NPOE (66 mg)/PVC (33 mg) and TDMACl (0.4 mg)/*o*-NPOE (66 mg)/PVC (33 mg)).

Anion	F ⁻	Cl ⁻	NO ₃ ⁻	SCN ⁻	Salicylate	ClO ₄ ⁻
log(β)	12.8	9.26	7.31	5.76	5.71	4.60

ty pattern, fluoride provides strongest binding constant with Sc(III)OEP (i.e., $\beta = 10^{12.8}$). However, the sequence of anion-ionophore binding based on the binding constant (i.e., F⁻ > Cl⁻ > NO₃⁻ > SCN⁻ > Salicylate > ClO₄⁻) is different from the sequence based on the selectivity data. Because the potentiometric response toward any anion is governed not only by the strength of binding with the ionophore but also by the partitioning of that anion into the hydrophobic membrane, the selectivity coefficient

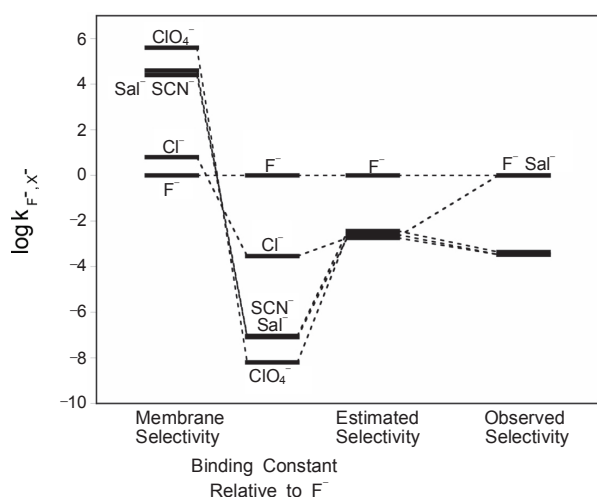


Figure 5. Comparison between estimated and experimentally observed potentiometric selectivity coefficients. Estimated coefficients are calculated based on the membrane selectivities and binding constants.

of the membrane can be conceptually described by:

$$k_{F^-, anion} = \left(\begin{array}{c} \text{selectivity} \\ \text{by membrane} \end{array} \right) \times \left(\begin{array}{c} \text{selectivity} \\ \text{by ionophore} \end{array} \right) \quad (4)$$

$$= \frac{p_{anion}}{p_{F^-}} \times \frac{\beta_{anion}}{\beta_{F^-}}$$

where p indicates partitioning coefficients of the given ion into the membrane. This equation indicates that the observed selectivity of the membrane can be described in terms of the membrane selectivity (i.e., Hofmeister selectivity series²⁷) and the ionophore selectivity (i.e., the binding constant). In Figure 5, the first column on the left is selectivity coefficients of a film doped only with TDMACl, which reflects the Hofmeister selectivity series. The second column illustrates the ratio of binding constants of anions to that of fluoride determined by the sandwich membrane method. By combining the first and second column based on Eq. (4), the third column is generated as an estimated selectivity coefficient. The column on the far right illustrates the experimentally observed potentiometric selectivity coefficients. The estimated selectivity pattern and the observed selectivity pattern matches reasonably well. The only exception is salicylate. In case of salicylate, highly favored partitioning of salicylic acid into the membrane seems to be responsible to the underestimation of the binding constant for salicylate.

Effect of dimerization. Metalloporphyrin-based anion sensors sometimes exhibit super-Nernstian responses. For example, fluoride sensors based on Ga(III) porphyrins, Zr(IV) porphyrins, and the chloride sensor based on In(III) porphyrins yielded much higher response slope (e.g., $-60 \sim -110$ mV/decade) than the Nernstian slope (i.e., 59.1 mV/decade).^{6-8,21} This has been explained by the formation of hydroxo-bridged dimer, L_2OH^+ in the membrane.²¹ The formation of L_2OH^+ changes the concentration of L^+ in the membrane since the total concentration of cationic species should be same as that of the lipophilic anionic sites due to the charge neutrality condition. The super-Nernstian responses is the consequence of increasing the concentration

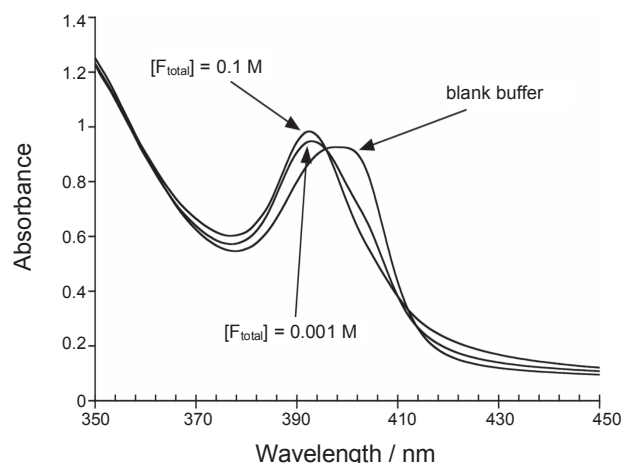


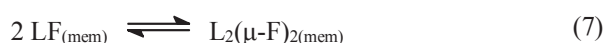
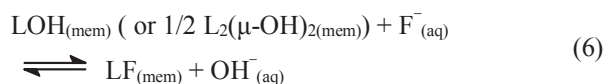
Figure 6. UV-vis spectra of the film (Sc(III)OEP/KTpCIPB (40 mol %)/*o*-NPOE/PVC) upon fluoride responses. In the presence of fluoride, a bis- μ -fluoro-dimer (390 nm) is observed.

of the charged carrier, L^+ , when the hydroxo-dimer is broken into monomers:



The increase of L^+ decreases the free concentration of anion (e.g., fluoride) in the Eq. (3) especially when the anionic sites are about 20 mol % to the total ionophore concentration. Thus, with a_{F^-} increasing and $[X^-]_{mem}$ decreasing, the increase of the logarithmic term (i.e., $\log [a_{F^-} / [X^-]_{mem}]$) in Eq. (1) is much higher. Therefore, a potential change greater than the theoretical slope is observed in Eq. (1).

Sc(III)OEP is also known to form a dimeric species not only with hydroxide but also with fluoride. Its dimeric form, $[Sc(III)OEP]_2(\mu-X)_2$ ($X = OH^-$ or F^-) has been confirmed *via* X-ray crystallography.¹⁶ This uncommon dimer form of $[Sc(III)OEP]_2(\mu-F)_2$ can be monitored *via* the UV-vis spectra of the membrane containing Sc(III)OEP and 40 mol % of KTFPB, and this is illustrated in Fig. 6. This figure shows the hypsochromic shift of the Soret band when the film is bathed in the 0.1 M fluoride solution. The characteristic spectral behavior of dimerization²⁸ as discussed in the previous study of Sc(III)OEP for the optical sensor is clearly observed.¹⁶ Therefore, fluoride facilitates formation of a dimer rather than breaking the dimer:



The initial form of Sc(III)OEP-OH seems to be a mixture of the dimer and the monomer based on the broad Soret band of the film in the buffer solution in Fig. 6. In reaction (6), as the activity of fluoride in the aqueous solution increases, fluoride gets into the membrane by an anion-exchange process and re-

places hydroxide in the monomeric and dimeric form of Sc(III)OEP. In reaction (7), fluoride-ligated Sc(III)OEP is now in equilibrium as a dimer and monomer, where the dimeric form is dominant for the given membrane condition.

It may seem inconsistent that Sc(III)OEP-doped membranes do not exhibit super-Nernstian EMF response even though dimer formation occurs as fluoride ion activity in the sample increases. Unlike hydroxo-bridged dimers of Ga(III), In(III), and Zr(IV) porphyrins, the fluoride-bridged dimer of Sc(III)OEP is a neutral species. Since this neutral dimer is formed from the neutral form of monomer in reaction (7), the formation and cleavage of dimer does not alter the concentration of the charged species, L^+ , in the membrane in Eq. (3). Therefore, super-Nernstian response is not observed.

Differential-type disposable HF sensor. The standard semiconductor cleaning process and some of industrial glass etching processes involves a treatment with hydrofluoric acid (HF) solution. For the preparation of a desired concentration of HF solution from the concentrated HF stock solution (usually 50 wt % HF in H_2O), the conductivity and/or pH is measured to calculate the concentration of HF. The direct measurement of fluoride level with a fluoride-selective electrode is not feasible because the activity of the free fluoride (pK_a 3.17) in the acidic solution is highly dependent on pH. Furthermore, at a pH much lower than 3, the major form of fluoride is HF, a neutral gaseous species, to which any ion-selective electrode is insensitive unless its presence generates a detectable ion. In this work, the quantification of HF in a solution (0.5 ~ 2.5 wt % HF in H_2O) is demonstrated with a fluoride-selective electrode based on Sc(III)OEP.

In order to overcome limitations of ion-selective electrode in detecting HF, a differential-type gas sensor is devised for the direct HF measurement. As can be seen in Fig. 7, two identical polymeric membrane fluoride-selective electrodes are prepared based on Sc(III)OEP. Only differences between two electrodes are the thickness and viscosity of the membrane; the thickness of the dried membrane at the working electrode is 15 μm ($\sigma = 2 \mu m$, $n = 7$), whereas the membrane thickness at the reference electrode is 65 μm ($\sigma = 2.3 \mu m$, $n = 7$). In addition, the ratio of PVC to *o*-NPOE is 1:2 and 2:1 for the working and the reference electrodes, respectively to make the reference membrane more viscous. In this configuration, the overall response can be described as:

$$\Delta E_{tot} = E_{working, outer} - E_{working, inner} - (E_{reference, outer} - E_{reference, inner}) \quad (8)$$

where ΔE_{tot} indicate the overall potential observed by a potentiometer. E is denoted for the boundary potential at either the outer interface or the inner interface of membrane of each electrode. In the conventional ion-selective electrode, only $E_{working, outer}$ is considered since other E terms are constant. However, in the differential HF sensor, not only the outer phase boundary potentials ($E_{working, outer}$ and $E_{reference, outer}$) but also the inner boundary potentials ($E_{working, inner}$ and $E_{reference, inner}$) should be considered since the diffusion of HF into the inner hydrogel layer changes inner boundary potentials (by changing activity of fluoride on the back side of the membrane). Now that two membranes are contacting

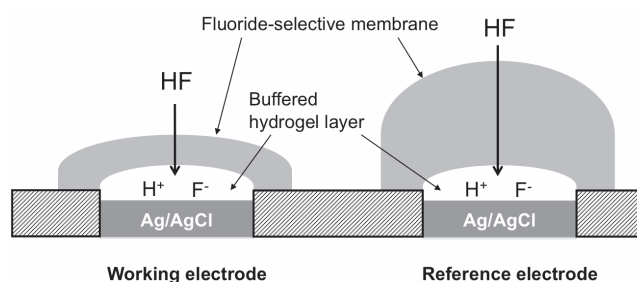


Figure 7. Schematic diagram of a differential-type HF sensor. Fluoride-selective membrane consists of Sc(III)OEP-OH/ KTpCIPB (40 mol %)/ PVC/*o*-NPOE. The inner hydrogel layer is formed by dispensing an aqueous mixture of PVP K90 (0.1 wt %), citric acid (1.0 M), and NaCl (0.1 M) on the Ag/AgCl electrode.

the exactly same solution and the membrane composition is basically identical except for the viscosity, the response at the outer boundary of the working electrode ($E_{working, outer}$) and the reference electrode ($E_{reference, outer}$) are equal. So Eq. (8) is reduced to:

$$\Delta E_{tot} = -E_{working, inner} + E_{reference, inner} \quad (9)$$

The boundary potential at inner layer can be changed by the gaseous HF which diffuses through the plasticized membrane, dissociates into a proton and a fluoride, and then increases the activity of fluoride in the inner hydrogel layer. The pH at the inner layer should be buffered by incorporating an appropriate buffer (i.e., citric acid). The pH of the cocktail solution for the inner hydrogel layer was adjusted to 4.9 so that when the sensor is hydrated in the conditioning solution (i.e., 1 M NaCl solution), the pH of inner layer is close to this pH and HF can be dissociated into fluoride without decreasing pH. Because the membrane at the working electrode is thinner and less viscous than that of the reference membrane, the accumulation of fluoride inside the working electrode is faster than inside the reference electrode. Therefore, depending on the HF level in the sample solution, the positive increase of EMF signal is observed.

Figure 8 shows the HF-dependent potential change with time at the working electrode (Fig. 8(a)) and the reference electrode (Fig. 8(b)). There are two evident processes that affect the potential of the membrane. As soon as the membrane is immersed in the sample solution, the potential changes during the hydration of the membrane and inner electrolyte/buffer layer. With the blank sample, the signal is stabilized within 30 seconds. With samples with HF, the diffusion of HF increases fluoride in the hydrogel layer inside the membrane and the anionic response is developed at this inner boundary. As a result, the increase of potential is observed. The rate of the potential change depends on the concentration of HF in the solution and the thickness of the membrane. As can be seen in Fig. 8(a), the rate of the potential change is proportional to the concentration of HF in sample and the potential at 180 seconds is also proportional to it. However, the reference electrode that consists of much thicker membrane shows the reduced potential change than the working electrode. Therefore, the difference of the working and the reference

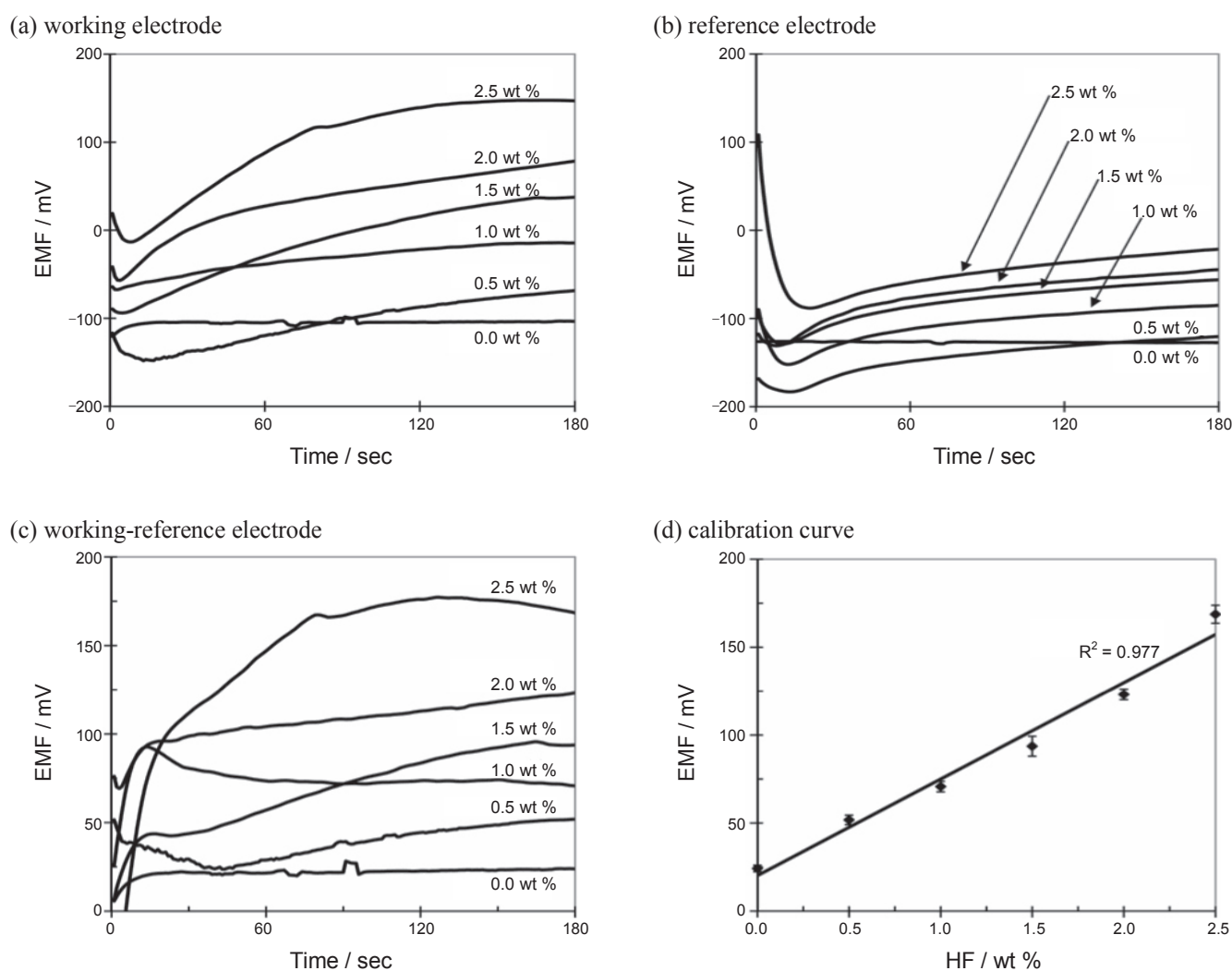


Figure 8. Responses to HF solution at various concentrations (0 ~ 2.5 wt%) by the working electrode (a) and by the reference electrode (b). Potential differences between the working and the reference electrode at each concentration are plotted in (c). EMF values at 180 seconds are used to build the calibration curve in (d).

electrode shows the increase of potential as HF increases in Fig. 8(c). Even though differences of potentials do not show linearity before 120 seconds, signals eventually reach a quasi-steady state and the reproducible linear EMF response is obtained at 180 seconds. Figure 8(d) shows the corresponding calibration curve which is linear ($R^2 = 0.977$) with a slope of 54.8 mV/wt %. This result clearly demonstrates the ability of the disposable-type differential fluoride sensor to monitor the content of HF in the aqueous sample.

A cheap and mass-producible screen-printed electrode was employed for the differential HF sensor since a quality control process in the manufacturing facility can yield highly reproducible electrochemical sensors so that it is not necessary to calibrate every individual sensor before use. For example, the glucose sensor strip based on this technology is available commercially with a high reliability that is sufficient for the use based on the sampling calibration method.²⁹ Further study on the differential-type fluoride sensor will lead to such a sensor that is directly used for the HF measurement in any acidic medium.

Conclusions

A fluoride selective electrochemical sensor based on the Sc(III)OEP ionophore has been evaluated in terms of selectivity, reversibility, response time, and lifetime. The lower detection limit of the optimized sensor for fluoride is about $10^{-4.5}$ M. The selectivity for fluoride over ClO_4^- , SCN^- , NO_3^- , Br^- , Cl^- is quite high. Only salicylate is a major interference. The binding constants with Sc(III)OEP and various anions have been measured by the sandwich membrane method, and results indicate a high binding constant for fluoride ($\beta_{\text{Sc(III)OEP-F}} = 10^{12.8}$). A simple demonstration of the detection of the neutral HF species in the acidic solution with this highly selective fluoride sensor was performed successfully using a novel differential gas sensing configuration.

Acknowledgments. We greatly acknowledge the National Institute of Health for supporting this work (EB-000784). G. S. Cha also gratefully acknowledges the financial support from

Kwangwoon University in 2008. This work is also supported by the National Research Foundation of Korea Grant funded by the Korean Government [NRF-2009-351-C00037].

References

1. Harrison, P. T. C. *J. Fluorine Chem.* **2005**, *126*, 1448.
2. Ayoob, S.; Gupta, A. K. *Crit. Rev. Environ. Sci. Technol.* **2006**, *36*, 433.
3. Simonian, A. L.; Grimsley, J. K.; Flounders, A. W.; Schoeniger, J. S.; Cheng, T. C.; Defrank, J. J.; Wild, J. R. *Anal. Chim. Acta* **2001**, *442*, 15.
4. Viveros, L.; Paliwal, S.; McCrae, D.; Wild, J.; Simonian, A. *Sens. Actuators B* **2006**, *115*, 150.
5. Zhan, C.-G.; Dixon, D. A. *J. Phys. Chem. A* **2004**, *108*, 2020.
6. Steinle, E. D.; Schaller, U.; Meyerhoff, M. E. *Anal. Sci.* **1998**, *14*, 79.
7. Malinowska, E.; Gorski, L.; Meyerhoff, M. E. *Anal. Chim. Acta* **2002**, *468*, 133.
8. Gorski, L.; Meyerhoff, M. E.; Malinowska, E. *Talanta* **2004**, *63*, 101.
9. Mitchell-Koch, J. T.; Malinowska, E.; Meyerhoff, M. E. *Electroanalysis* **2005**, *17*, 1347.
10. Gorski, L.; Saniewska, A.; Parzuchowski, P.; Meyerhoff, M. E.; Malinowska, E. *Anal. Chim. Acta* **2005**, *551*, 37.
11. Badr, I. H. A.; Meyerhoff, M. E. *J. Am. Chem. Soc.* **2005**, *127*, 5318.
12. Badr, I. H. A.; Meyerhoff, M. E. *Anal. Chim. Acta* **2005**, *553*, 169.
13. Badr, I. H. A.; Meyerhoff, M. E. *Anal. Chem.* **2005**, *77*, 6719.
14. Mitchell-Koch, J. T.; Pietrzak, M.; Malinowska, E.; Meyerhoff, M. E. *Electroanalysis* **2006**, *18*, 551.
15. Wang, L.; Meyerhoff, M. E. *Anal. Chim. Acta* **2008**, *611*, 97.
16. Kang, Y.; Kampf, J. W.; Meyerhoff, M. E. *Anal. Chim. Acta* **2007**, *598*, 295.
17. Gouterman, M.; Holten, D.; Lieberman, E. *Chem. Phys.* **1977**, *25*, 139.
18. Arnold, J.; Hoffman, C. G.; Dawson, D. Y.; Hollander, F. J. *Organometallics* **1993**, *12*, 3645.
19. Meier, P. *Anal. Chim. Acta* **1982**, *136*, 363.
20. Bakker, E.; Bühlmann, P.; Pretsch, E. *Chem. Rev.* **1997**, *97*, 3083.
21. Steinle, E. D.; Amemiya, S.; Bühlmann, P.; Meyerhoff, M. E. *Anal. Chim. Acta* **2000**, *422*, 5766.
22. Eugster, R.; Rosatzin, T.; Rusterholz, B.; Aebersold, B.; Pedrazza, U.; Ruegg, D.; Schmid, A.; Spichiger, U. E.; Simon, W. *Anal. Chim. Acta* **1994**, *289*, 1.
23. Sears, J. K.; Darby, J. R. *The Technology of Plasticizers*; John Wiley & Sons, Inc.: New York, 1982; p 989.
24. Dielectric constant of DTDA is not known to author but estimated based on dielectric constants of didodecyl adipate (2.59) and dioctadecyl adipate (2.47).
25. Mi, Y. M.; Bakker, E. *Electrochem. Solid-State Lett.* **2000**, *3*, 159.
26. Qin, Y.; Bakker, E. *Talanta* **2002**, *58*, 909.
27. Hofmeister, F. *Arch. Exp. Pathol. Pharmacol.* **1888**, *24*, 247.
28. Tranthi, T. H.; Lipskier, J. F.; Maillard, P.; Momenteau, M.; Lopez-castillo, J. M.; Jaygerin, J. P. *J. Phys. Chem.* **1992**, *96*, 1073.
29. <http://www.i-sens.com/product/smbg.htm>